HHS Public Access

Author manuscript

Nano Lett. Author manuscript; available in PMC 2019 December 01.

Published in final edited form as:

Nano Lett. 2019 November 13; 19(11): 8333–8341. doi:10.1021/acs.nanolett.9b04147.

Sustained delivery of carfilzomib by tannic acid-based nanocapsules helps develop antitumor immunity

Maie S. Taha[1,2], **Gregory M. Cresswell**[3], **Joonyoung Park**[1], **Wooin Lee**[4], **Timothy L. Ratliff**[3], **Yoon Yeo**[1,5,*]

[1]Department of Industrial and Physical Pharmacy, Purdue University, 575 Stadium Mall Drive, West Lafayette, IN 47907, USA

[2]Department of Pharmaceutics and Industrial Pharmacy, Faculty of Pharmacy, Cairo University, Cairo 11562, Egypt

[3]Department of Comparative Pathobiology and Purdue University Center for Cancer Research, 625 Harrison Street, West Lafayette, IN, 47907, USA

[4]College of Pharmacy and Research Institute of Pharmaceutical Sciences, Seoul National University, Seoul, 08826, Republic of Korea

[5]Weldon School of Biomedical Engineering, Purdue University, West Lafayette, IN 47907, USA

Abstract

A group of chemotherapeutic drugs has gained increasing interest in cancer immunotherapy due to the potential to induce immunogenic cell death (ICD). A critical challenge in using the ICD inducers in cancer immunotherapy is the immunotoxicity accompanying their antiproliferative effects. To alleviate this, a nanocapsule formulation of carfilzomib (CFZ), an ICD-inducing proteasome inhibitor, was developed using interfacial supramolecular assembly of tannic acid (TA) and iron, supplemented with albumin coating. The albumin-coated CFZ nanocapsules (CFZ-pTA-alb) attenuated CFZ release, reducing toxicity to immune cells. Moreover, due to the adhesive nature of TA assembly, CFZ-pTA-alb served as a reservoir of damage-associated molecular patterns released from dying tumor cells to activate dendritic cells. Upon intratumoral administration, CFZ-pTA-alb prolonged tumor retention of CFZ and showed consistently greater antitumor effects than cyclodextrin-solubilized CFZ (CFZ-CD) in B16F10 and CT26 tumor models. Unlike CFZ-CD, the locally injected CFZ-pTA-alb protected or enhanced $CD8^+$ T cell population in tumors, helped develop splenocytes with tumor-specific interferon-γ response, and delayed tumor development on the contralateral side in immunocompetent mice (but not in athymic nude mice), which support that CFZ-pTA-alb contributed to activating antitumor immunity. This study demonstrates that sustained delivery of ICD inducers by TA-based nanocapsules is an effective way of translating local ICD induction to systemic antitumor immunity.

*Corresponding author: Yoon Yeo, Ph.D., Phone: 1.765.496.9608, Fax: 1.765.494.6545, yyeo@purdue.edu.

Supporting Information Available: Materials and Methods, Supporting Figures and Tables are available free of charge *via* the Internet at http://pubs.acs.org.

Keywords

Immunogenic cell death; carfilzomib; nanocapsules; tannic acid; sustained release

Chemotherapy is one of the main cancer treatments along with surgery, radiation and immunotherapy. Chemotherapeutic drugs interfere with the growth of tumor cells by damaging or blocking the synthesis of nucleic acids, preventing cell division, or inhibiting homeostatic control of regular cellular functions. Some of the chemotherapeutic drugs have gained increasing interest as immunogenic cell death (ICD) inducers. ICD-inducing chemotherapy kills tumor cells such that it induces the production of tumor-associated antigens and damage-associated molecular patterns (DAMPs), thereby helping the host to develop adaptive immunity to the tumor cells.[1] Therefore, ICD inducers can play an important role in cancer immunotherapy as standalone therapeutics to induce specific anti-tumor immune responses[2] as well as companion drugs to enhance the effect of immune checkpoint blockade therapy.[3]

Several existing chemotherapeutic drugs are identified to be ICD inducers, which include anthracyclines (doxorubicin, idarubicin, epirubicin), mitoxantrones, oxaliplatin, cyclophosphamide, bortezomib, and paclitaxel.[4, 5] In addition, carfilzomib (CFZ), a second-generation proteasome inhibitor, is considered an emerging ICD inducer,[6] with improved efficacy and safety profiles over the first-generation bortezomib.[7-9] CFZ irreversibly inhibits the proteolytic activity of the proteasome[9] and prevents the degradation of misfolded and other key signaling proteins, causing a significant endoplasmic reticulum (ER) stress,[10, 11] the main mechanism of ICD induction.[6] Therefore, it is expected that CFZ delivered to tumors may produce a spatially defined set of tumor-associated antigens and DAMPs, i.e., *in situ* tumor vaccines and endogenous immune adjuvants.

However, a critical challenge in using chemotherapeutic agents to promote cancer immunotherapy is that their antiproliferative effects damage not only tumor cells but also immune cells in the tumor microenvironment, impairing their ability to mount immune responses to dying tumor cells.[12, 13] Given the paradoxical effect of chemotherapy, it is recognized that the regimen needs to be optimized to maximize its therapeutic benefit in the context of cancer immunotherapy.[14] In fact, compared to the standard maximum tolerated dose (MTD) regimen, prolonged administration of low doses of chemotherapeutics, called metronomic chemotherapy, has shown reduced immunotoxicity, thereby improving antitumor efficacy.[15] Moreover, metronomic dosing of chemotherapeutics can selectively deplete immunosuppressive cell populations, such as myeloid-derived suppressor cells and regulatory T cells, from the tumor microenvironment.[16-18] These studies suggest that sustained delivery of ICD inducers to tumors may protect antitumor immune cells and help them to develop effective tumor-specific immune responses.[16]

Nanoparticles (NPs) have been widely pursued in the delivery of chemotherapeutics. They have been used to help disperse water-insoluble drugs and/or protect metabolically labile drugs from the hostile physiological environments.[19] NPs may be designed to control the drug release rate over a prolonged period, facilitating metronomic delivery of chemotherapeutics.[20] In addition, a recent study reports that NPs can capture tumor

neoantigens and DAMPs from dying tumor cells and, as a favored substrate of phagocytes,[21] facilitate their delivery to dendritic cells to activate the antitumor immunity.[22] Therefore, NPs may provide multiple benefits to the delivery of ICD inducers: First, NPs can control the release of ICD inducers to prevent damaging immune cells involved in antitumor immunity. Second, with the relatively large size and drug release control, NPs can retain a drug in tumors longer than the free drug counterpart. Third, NP residuals may capture the tumor-associated antigens and DAMPs produced by dying tumor cells, improving their exposure to antigen presenting cells.

In the present study, we develop a nanocapsule formulation of CFZ, which can retain the drug in tumors for a prolonged period, control the drug release, and serve as a reservoir of tumor antigens and DAMPs. We hypothesize that a prolonged delivery of CFZ puts tumor cells under extended ER stress to induce ICD,[6, 23-25] while minimizing damages to chemosensitive immune cells recruited to tumors. In addition, nanocapsules capturing tumor antigens and DAMPs may enhance their delivery to dendritic cells (DCs) and activation of the cells. For this purpose, we encapsulate CFZ in a supramolecular assembly of tannic acid (TA) and iron[26] and modified the surface with albumin (CFZ-pTA-alb) to control the drug release. We envision that locally (intratumorally) injected CFZ nanocapsules will activate antitumor immune responses, which can translate to systemic protection against tumors. We evaluate the ability of CFZ nanocapsules to control the drug release and capture soluble proteins released from dying tumor cells. We then compare the effects of CFZ nanocapsules and unformulated CFZ on tumor cells and immune cells *in vitro* and evaluate how they control tumor growth and help develop local and systemic antitumor immunity using mouse models of B16F10 and CT26 tumors.

CFZ-pTA nanocapsules were prepared by interfacial assembly of TA-iron complexes[26] (Figure 1a). An ethanolic solution of tannic acid and concentrated CFZ was added to an aqueous Fe^{3+} solution. TA and Fe^{3+} formed an instantaneous supramolecular assembly at the interface between ethanol and water, making spherical nanocapsules in which CFZ undergoes supersaturation and formation of nanoclusters with concomitant solvent exchange. The CFZ-containing nanocapsules (CFZ-pTA) had an average diameter of 100-200 nm (Figure 1b; Table S1). The unique dark blue color of the mixture indicated the formation of TA and Fe^{3+} (pTA) complexes (Figure S1a). The pTA shell was clearly seen after etching of CFZ core (Figure 1b). The shell was distinguished from pTA complexes assembled in the absence of CFZ (Figure S1b), indicating that the pTA assembly in CFZ-pTA is mainly present on the surface of CFZ nanoclusters. The z-average of CFZ-pTA nanocapsules measured by DLS was 164 ± 1 nm (Table S1). Their surface charge was measured to be −27 ± 4 mV (Table S1), reflecting the deprotonated catechol hydroxyl groups of the surface pTA. Interestingly, an ethanolic solution of concentrated CFZ (without TA and $FeCl_3$), mixed with water, also formed nanoclusters with a similar size as CFZ-pTA (Figure S1c). The CFZ nanoclusters, unlike CFZ-pTA, showed positive charge in water (Table S1), reflecting protonated nitrogens of CFZ. However, the unprotected CFZ nanoclusters immediately aggregated in phosphate buffer (10 mM, pH 7.4), where the buffer ions neutralized the positive surface charges (Table S1). In contrast, CFZ-pTA maintained the size in phosphate buffer, indicating the protective effect of pTA assemblies on the nanocluster surface. CFZ-pTA also showed stable particle size in 50% FBS over 24 h

(Figure S2a) maintaining the spherical structure (Figure S3). This suggests that pTA shell should be stable enough to protect the CFZ-pTA in circulation from disintegration or aggregation. The CFZ content in CFZ-pTA was 51 ± 1 wt% and the TA content 49 ± 7 wt% (Table S2).

CFZ-pTA was further modified with albumin by 4 h incubation in 2 mg/mL albumin solution. The albumin-coated CFZ-pTA nanocapsules (CFZ-pTA-alb) was similar in size to CFZ-pTA (Figure 1b; Table S1) but slightly less charged due to the albumin coverage (Table S1). The albumin content was estimated to be 15 ± 1 wt% of CFZ-pTA-alb (Figure S4; Table S2) and the CFZ content 41 ± 2 wt% (Table S2). CFZ-pTA-alb showed colloidal stability in 50% FBS (Figure S2b), similar to CFZ-pTA.

To evaluate the effect of albumin coating on CFZ release control, CFZ-pTA and CFZ-pTA-alb were compared with respect to their CFZ release kinetics *in vitro*. The particles were first housed in photocrosslinkable polyethyleneglycol dimethylacrylate (PEGDA) hydrogel and incubated in 10% FBS-supplemented RPMI 1640 medium, which was sampled at regular intervals to quantify the released CFZ. The hydrogel method was used in lieu of common centrifugation or dialysis methods to avoid the risk of pressurizing and destroying nanocapsules during the repeated centrifugation or excessively diluting the drug to below the detection limit.[27] The hydrogel confines particles and helps separate them from the medium and does not require a large volume of medium for incubation.[28] However, the drug release rate measured by this method does not necessarily reflect the actual rate because the hydrogel also functions as a barrier to drug diffusion; thus, the results are only meaningful for rank ordering the two particles. CFZ-pTA-alb showed slower drug release than CFZ-pTA: in 24 h, 5% and 10% of CFZ was released from CFZ-pTA-alb and CFZ-pTA, respectively (Figure 2a), indicating that albumin coat served as an additional barrier to CFZ release from the particles. CFZ is known for high plasma protein binding (97.6–98.2%)[29, 30]; therefore, it is conceivable that CFZ escaping CFZ-pTA-alb was temporarily trapped with the surface-bound albumin. A similar result was shown with mitoxantrone-loaded pullulan NPs,[31] where the delayed release of mitoxantrone from albumin-bound NPs was explained by the high affinity of the drug for the surface-bound albumin.[32]

The stable CFZ encapsulation also enhanced the metabolic stability of CFZ, an epoxyketone peptide, which degrades quickly by peptide cleavage and epoxide ring opening.[29] Metabolic stability of CFZ in CFZ-pTA-alb, CFZ-pTA, and CFZ-CD (CFZ solubilized with 2-hydroxypropyl-β-cyclodextrin (CD), a solubilizing agent,[33] as in the commercial product) was compared *in vitro* after 30 min incubation in whole blood, which contain epoxide hydrolases/peptidases.[29] With CFZ-CD, 66.0 ± 4.0% of total CFZ was recovered after the incubation. CFZ-pTA and CFZ-pTA-alb displayed much improved metabolic stability, with 74.1 ± 7.8% and 91.8 ± 6.6% of CFZ, respectively, surviving the same condition (Figure 2b). This result suggests the protective functions of pTA. The additional protection offered by the albumin coat is consistent with the differential *in vitro* drug release kinetics (Figure 2a).

The sustained CFZ release from CFZ-pTA(-alb) manifested as delayed cytotoxicity in cancer cell lines. B16F10 (melanoma) cells and HCC-1937 (triple negative breast cancer) were

treated with unformulated CFZ (solubilized in DMSO), CFZ-pTA, and CFZ-pTA-alb in different concentrations. With 2 h exposure, both CFZ-pTA and CFZ-pTA-alb showed minimal toxicity compared to the unformulated CFZ (Figure 2c; Figure S5a). With extended exposure, nanocapsules gradually caught up with the unformulated CFZ to show comparable cytotoxicities after 72 h exposure (Figure 2d, Figures S5 and S6). The attenuation of cytotoxicity was more pronounced with CFZ-pTA-alb (Figure 2d, Figures S5 and S6). Blank pTA or blank pTA-alb showed minimal toxicity in B16F10 cells[34] at concentrations equivalent to CFZ nanocapsules, with 84% (pTA) and 76% (pTA-alb) viability, after maximum exposure (the highest concentration and 72 h incubation) (Figure S7). This indicates that cytotoxicity of the nanocapsules is mainly due to CFZ rather than the carriers. There were little signs of cellular uptake of CFZ-pTA or CFZ-pTA-alb (Figure S8), indicating that the differential cytotoxicity reflects the extent of CFZ release outside the cells during the indicated incubation periods. The greater delay in cytotoxicity of CFZ-pTA-alb relative to CFZ-pTA is consistent with their difference in *in vitro* drug release and stability in whole blood.

To estimate whether the sustained supply of CFZ is beneficial to sparing immune cells such as lymphocytes and DCs in the tumor microenvironment, we tested the cytotoxic effect of CFZ on splenocytes and bone marrow-derived DCs (BMDCs) in two treatment regimens (Figure 3a): a pulse treatment of bolus dose (bolus-pulse) and an extended treatment of low dose (low-extended), where bolus-pulse indicates incubation of cells in different CFZ concentrations for 2.4 h followed by washout and incubation in drug-free medium for additional 21.6 h making the total incubation time of 24 h, and low-extended indicates incubating cells in $1/10^{th}$ CFZ concentrations for 24 h. The bolus-pulse regimen represents unformulated CFZ that is immediately available to the tumor upon intratumoral injection but rapidly diffuses to the circulation, whereas the low-extended regimen mimics the sustained release of CFZ from CFZ-pTA-alb over a prolonged period of time. Lymphocytes and DCs were chosen as representative immune cells that play key roles (antigen presentation, antigen-specific cytotoxicity) in adaptive antitumor immunity. Splenocytes freshly harvested from C57BL/6 mice were used as a surrogate for lymphocytes, as the spleen is the largest secondary lymphoid organ containing 25% of total lymphocytes,[35] where B cells and T cells constitute 45-50% and 30-35%, respectively.[36] Splenocytes were less sensitive to the low-extended regimen than to the bolus-pulse regimen (Figure 3b; Figure S9a). A similar trend was seen with BMDCs (Figure 3c; Figure S9b). In contrast, B16F10 cells were equally sensitive to the two regimens (Figure 3d; Figure S9c). The selective tolerance of DCs and lymphocytes to a low dose CFZ supplied over an extended period is likely due to the overexpression of P-gp efflux proteins on those cells.[37-39] As a P-gp substrate,[40] CFZ may be efficiently excluded by the immune cells at a relatively low dose but not at a high dose that saturates the efflux machinery. These results suggest that the sustained supply of CFZ in the tumor microenvironment, while equally effective against tumor cells as a bolus treatment, be beneficial to protecting immune cells in tumor microenvironment.

DCs take up tumor antigens, deliver them to draining lymph nodes (DLNs), where they cross-present them to activate T-lymphocytes. A previous study reported that polymeric NPs captured neoantigens and DAMPs of dying tumor cells and delivered them to DCs in DLNs.[22] A fraction of CFZ-pTA-alb that remains in the extracellular space of tumors, may provide

a similar function via the underlying pTA layer, which can interact with proteins via hydrogen bonding and hydrophobic interactions.[41, 42] To test if CFZ-pTA-alb captures tumor-associated antigens and/or DAMPs, we incubated the nanocapsules in the medium containing soluble proteins released from CFZ-killed B16F10 cells and analyzed the surface-bound proteins. LC-MS/MS analysis showed a large amount of mouse proteins, several of which were identified to be DAMPs (Calreticulin, Histone H2A.Z, Histone H1.5, Histone H1.3, Histone H1.4, Histone H3.1, Histone H4, Heat shock 70 kDa protein 4, Heat shock protein HSP 90-α, Heat shock protein HSP 90-β),[22] captured by CFZ-pTA-alb (Figure 4a; Figure S10).

We next examined whether the DAMP-adsorbed nanocapsules increased DC activation. BMDCs were incubated with B16F10 cells pretreated with CFZ, CFZ-pTA-alb or blank-pTA-alb (vehicle) to assess their expression of CD40 and CD86 (DC activation markers) upon their interaction. An excess dose of CFZ (10 μM CFZ equivalent) was used to maximize the effect on B16F10 cells, and the cells were briefly rinsed to remove the extra drug prior to the incubation with BMDCs. Untreated or blank pTA-alb-treated (i.e., healthy) B16F10 cells induced no increase in CD40 or CD86 expression in BMDCs. CFZ and CFZ-pTA-alb-treated B16F10 cells increased the expression of the two activation markers, with CFZ-pTA-alb showing a more prominent effect than CFZ (Figures 4b and 4c). The DC activation by CFZ-treated B16F10 cells supports the potential of CFZ as an ICD inducer. The relatively high response to CFZ-pTA-alb-treated cells suggest that nanocapsules, which were not removed during the rinsing step, may have helped to increase local exposure of DAMPs to DCs. Therefore, in addition to the primary role of CFZ delivery, CFZ-pTA-alb staying in extracellular matrix of tumors may capture DAMPs from dying cells and deliver them to DCs to enhance their activation.

We examined if DC activation correlates with its uptake of tumor antigens. B16F10 cells, stained with DiI (a lipophilic dye) and pretreated with CFZ, CFZ-pTA-alb or blank-pTA-alb (vehicle) for 24 h, were incubated with BMDCs for 4 or 24 h. BMDCs were identified by anti-CD11c antibody and analyzed by flow cytometry. Cells positive for both DiI and CD11c (DiI^+CD11c^+ cells) were considered the BMDCs taking up DiI-stained B16F10 cells and fragments of dying cells. With no apparent toxicity to B16F10 cells (Figure S7), blank-pTA-alb induced no increase in the BMDC uptake of the treated B16F10 cells (Figures 4d and 4e; Figure S11a). In contrast, CFZ or CFZ-pTA-alb-pretreated B16F10 cells induced greater extents of DiI^+CD11c^+ cells per total $CD11c^+$ cells (i.e., BMDCs uptake of DiI^+ B16F10 cells and their fragments) than the untreated B16F10 cells. The uptake of CFZ-pretreated B16F10 cells by BMDCs was diminished at 4 °C (Figure S11b), indicating that the uptake was an energy-dependent process, most likely phagocytosis. CFZ-pTA-alb-treatment induced a greater DiI^+CD11c^+ cells fraction than CFZ-treated cells, especially at early incubation (Figures 4d and 4e). Confocal microscopy found a consistent trend, where the BMDCs uptake of DiI^+ cells/fragments increased with CFZ pretreatment, more evidently with CFZ-pTA-alb, according to the Pearson's correlation coefficient of signal colocalization (Figures S12a and S12b). Staining of BMDC membranes demonstrated that CFZ-pTA-alb-treated B16F10 cells and fragments were completely internalized by BMDCs (Figure S12c). These results suggest that CFZ-pTA-alb pre-treatment facilitate tumor antigen delivery to DCs.

The *in vitro* results so far suggest that CFZ-pTA-alb can contribute to the generation of tumor-specific immunity by at least one of the three complementary mechanisms: (i) killing tumor cells to generate tumor-associated antigens by CFZ; (ii) sparing immune cells (such as T cells and DCs) by sustained release of CFZ; and (iii) serving as a reservoir of DAMPs to enhance the activation and antigen uptake of DCs. On the basis of these results, the effect of intratumorally injected CFZ-pTA-alb on tumor growth and its environment was evaluated in two syngeneic tumor models (B16F10@C57BL/6, CT26@Balb/c).

The antitumor effect of CFZ-pTA-alb was evaluated in B16F10 melanoma-bearing C57BL/6 mice and compared with the effect of CFZ-CD (CFZ solubilized with CD as in the commercial product). Subcutaneous B16F10 tumors were injected intratumorally once with PBS, CFZ-CD or CFZ-pTA-alb at a dose equivalent to CFZ 1.2 μg per mouse. With this regimen, CFZ-CD had no significant suppression of tumor growth as compared to PBS control (Figures 5a and 5b). However, CFZ-pTA-alb attenuated tumor growth showing significant difference from PBS and CFZ-CD in the specific growth rate (rate of exponential tumor growth calculated for each animal[43]) (Figures 5a and 5b). This contrasts with *in vitro* results, where the sustained drug release of CFZ-pTA-alb led to initial delay in cytotoxic effect (Figures 2c and d; Figures S5 and 6). This suggests that additional mechanisms account for the *in vivo* effects of CFZ-pTA-alb.

The superior effect of CFZ-pTA-alb may first be attributed to the prolonged tumor retention of CFZ in the form of nanocapsules due in part to the size and the metabolic stability (Figure 2b), thereby increased local availability of the drug. To test this, another group of identically treated animals were sacrificed 2 h after the treatment, and CFZ in tumors and plasma were quantified. The tumors and plasma were treated with Triton-X 100 to disassemble CFZ-pTA-alb and release CFZ. Therefore, the measured CFZ represents the total detectable amount of CFZ, including both free/released and encapsulated in CFZ-pTA-alb. The amount of CFZ retrieved from CFZ-pTA-alb-treated tumors was 3 times higher than that of CFZ-CD group (Figure 5c). The CFZ level in plasma showed the opposite trend, with the CFZ-CD group showing a higher level than that of CFZ-pTA-alb (Figure 5d). This result indicates that CFZ-CD, though available as soluble CFZ from the beginning, was rapidly cleared from the tumor, the scenario simulated by the bolus-pulse regimen *in vitro* (Figure 3). On the other hand, the relatively high level of total CFZ in CFZ-pTA-alb-treated tumors suggests that the nanocapsules were better retained in the tumor than CFZ-CD due to the delayed intratumoral transport and lymphatic drainage, making more drug available to tumors. In addition, due to the stability, CFZ-pTA-alb would have provided sustained CFZ exposure to tumor, the scenario represented by the low-extended regimen (Figure 3).

Given the benefit of sustained CFZ release in protecting immune cells predicted *in vitro* (Figures 3b and c and Figures S9a and 9b), we then measured $CD8^+$ T cell population in B16F10 tumors harvested at 7 days post-treatment. CFZ-CD-treated tumors apparently showed fewer $CD8^+$ T cells than PBS-treated tumors though statistical significance was not reached (Figure 5e), indicating toxicity of bolus CFZ-CD. In contrast, CFZ-pTA-alb-treated tumors had a comparable level of $CD8^+$ T cells to the PBS-treated tumors, suggesting difference from CFZ-CD-treated tumors (Figure 5e). This result is consistent with *in vitro*

prediction (Figures 3b and 3c and Figures S9a and S9b) and supports that sustained release of CFZ from CFZ-pTA-alb help spare tumor-infiltrating cytotoxic lymphocytes.

Considering the potential to spare and activate antitumor immune cells in the tumor microenvironment (Figures 3b and 3c; Figures 4b and 4c; Figure 5e; Figures S9a and S9b), we asked if the locally administered CFZ-pTA-alb would help develop adaptive immunity to tumors. To test this, we inoculated C57BL/6 mice with B16F10 cells on the flanks of both hind limbs with one-week interval and administered CFZ-pTA-alb (or CFZ-CD, PBS) to the first tumor (tumor A) intratumorally (Figure 6a). While following up the growth of tumor A, we also monitored the occurrence of tumor on the contralateral side (tumor B), which was left untreated, to observe the 'abscopal' effect due to systemic T-cell activation. Consistent with the previous experiment (Figures 5a and 5b), CFZ-pTA-alb attenuated the growth of the treated tumor more effectively than the other two treatments (Figures 6b and 6c). In addition, CFZ-pTA-alb delayed the emergence of tumor B, whereas CFZ-CD was no different from the PBS control (Figure 6d). To test whether the effect on tumor B was due to the systemic antitumor immunity or the drug entering the circulation from the injection site, the same test was performed on athymic nude mice with deficient T cell function (Figure S13a). B16F10-bearing nude mice showed similar responses in the first tumor A, where CFZ-pTA-alb suppressed tumor growth more effectively than the other two treatments (Figures S13b and S13c). On the other hand, CFZ-pTA-alb showed no difference from CFZ-CD or PBS in the occurrence of tumor B on the contralateral side (Figure S13d). This result supports that the effect of local application of CFZ-pTA-alb on the untreated distant tumor shown in the immunocompetent C57BL/6 mice is mediated by the activation of systemic T cell immunity.

To verify the generation of tumor-specific T-cell immunity, we performed immunophenotyping of the treated tumors and tumor DLNs and tested antigen-specific production of IFN-γ from splenocytes of the treated animals. B16F10 tumors are known to be poorly immunogenic with few tumor-infiltrating cytotoxic T cells[44] and, thus, difficult to obtain substantial readouts (Figure 5e). Therefore, we used the CT26 colon cancer model in syngeneic Balb/c mice, which is relatively more immunogenic due to the high mutational burden[45] and conducive to monitoring phenotypic changes in tumor immune microenvironment.[44, 46-48] CT26 tumors responded to intratumorally-administered treatments in a similar manner as B16F10 tumors, with CFZ-pTA-alb showing better effect than PBS or CFZ-CD (Figures 7a and 7b). In addition, the $CD8^+$ T cell populations in CT26 tumors and tumor DLNs of the CFZ-pTA-alb group were apparently higher than those of the CFZ-CD group (Figure 7c; Figure S14), consistent with B16F10 tumors (Figure 5e) except that the extents were overall higher. The abscopal effect of local treatment was also examined (Figure 8), but all mice (including PBS-treated ones) did not develop tumor B on the contralateral side, likely due to the concomitant immunity common to immunogenic tumors,[49, 50] and revealed no difference among the groups. Nevertheless, splenocytes collected from the mice at the conclusion of study (22 days post-treatment) showed a difference in response to AH1 peptide, a CT26 immunodominant MHC class-I restricted antigen.[51] Splenocytes collected from the CFZ-pTA-alb-treated mice showed increase in IFN-γ secretion upon the stimulation with AH1 peptide as compared to those incubated in PBS control (Figure 8d; Figure S15). In contrast, splenocytes from PBS or CFZ-CD-treated animals did not show significant difference in IFN-γ secretion with and without AH1

peptide stimulation. Of note, splenocytes of the PBS-treated mice produced a relatively high level of IFN-γ irrespective of antigen challenge, likely due to the uncontrolled tumor growth, which induces the accumulation of IFN-γ-producing cells in the spleen via soluble factors.[52, 53] This result supports that intratumoral administration of CFZ-pTA-alb, but not CFZ-CD, helps develop tumor-specific T-cell immunity, which can affect distant tumors.

This study has focused on the advantage of controlling CFZ release by CFZ-pTA-alb in sparing immune cells in the tumor microenvironment. The literature suggests that the sustained CFZ release in the tumor may have additional benefits. Chemotherapy based on MTDs tend to selectively target chemosensitive cancer cells, leaving behind chemoresistant cell populations that may lead to tumor relapse and emergence of drug resistance.[54] On the contrary, metronomic chemotherapy targets the tumor microenvironment and disengages tumor cells from its support system, resulting in long-lasting tumor regression.[16, 18, 54] In addition, sustained low doses of chemotherapeutics show antiangiogenic effects[55, 56] and avoid the induction of tumor-initiating cancer stem cells.[54] Bortezomib (the first-generation proteasome inhibitor) has shown to induce endothelial cell apoptosis and downregulate proteins responsible for the angiogenic phenotype in endothelial cells, such as vascular endothelial cell growth factor, interleukin-6, insulin-like growth factor-I, angiopoietin 1 and angiopoietin 2.[57, 58] The antiangiogenic effect was also reported with oprozomib, an orally active second-generation proteasome inhibitor.[59] As a proteasome inhibitor with a similar mechanism of action, CFZ may have an antiangiogenic effect likewise, which would manifest better with sustained release. The contribution of sustained CFZ delivery by CFZ-pTA-alb to antiangiogenesis is worth investigation.

In summary, we demonstrated the potential to translate local chemotherapy to systemic antitumor immunity via sustained induction of ICD. The sustained release of CFZ was achieved by encapsulation in nanocapsules made of TA/iron interfacial assemblies covered with albumin - CFZ-pTA-alb, which serve as effective diffusion barriers to CFZ. CFZ-pTA-alb showed consistently greater antitumor effects than CD-solubilized CFZ (CFZ-CD) *in vivo*, due to the enhanced metabolic stability and prolonged tumor retention of CFZ. In addition, the effects of local CFZ-pTA-alb administration on remote tumor growth, immune cell population in tumor microenvironment, and the response of splenocytes to a tumor antigen suggest that CFZ-pTA-alb played positive roles in activating antitumor immunity. Our results support that CFZ-pTA-alb enables the sustained cytotoxic effect to tumor cells with minimal damage to neighboring immune cells and may facilitate DC activation as a reservoir of DAMPs, providing the basis of immune activation. Therefore, CFZ-pTA-alb is an effective formulation to translate local ICD induction to systemic antitumor immunity.

Supplementary Material

Refer to Web version on PubMed Central for supplementary material.

Acknowledgments

This work was supported by the National Institutes of Health (R01 EB017791, R01 CA232419). We also acknowledge the fellowship support from the Egyptian Government Ministry of Higher Education Missions Sector to M.S.T. This work was also supported by the Indiana Clinical and Translational Sciences Institute, funded in part

by grant #UL1 TR001108 from the National Institutes of Health, National Center for Advancing Translational Sciences, Clinical and Translational Sciences Award. The LC-MS/MS analysis of proteins bound to nanocapsules was performed at the Purdue Proteomics Facility of the Bindley Bioscience Center.

References

1. Pol J; Vacchelli E; Aranda F; Castoldi F; Eggermont A; Cremer I; Sautès-Fridman C; Fucikova J; Galon J; Spisek R; Tartour E; Zitvogel L; Kroemer G; Galluzzi L OncoImmunology 2015, 4, (4), e1008866–e1008866. [PubMed: 26137404]
2. Aznar MA; Tinari N; Rullán AJ; Sánchez-Paulete AR; Rodriguez-Ruiz ME; Melero I The Journal of Immunology 2017, 198, (1), 31. [PubMed: 27994166]
3. Cui S Med Sci Monit 2017, 23, 3360–3366. [PubMed: 28697172]
4. Garg AD; Dudek-Peric AM; Romano E; Agostinis P Int J Dev Biol 2015, 59, (1-3), 131–40. [PubMed: 26374534]
5. Dmitri VK; Abhishek DG; Agnieszka K; Olga K; Patrizia A; Peter V Nature Reviews Cancer 2012, 12, (12), 860. [PubMed: 23151605]
6. Serrano-del Valle A; Anel A; Naval J; Marzo I Frontiers in Cell and Developmental Biology 2019, 7, (50).
7. Dick LR; Fleming PE Drug Discovery Today 2010, 15, (5), 243–249. [PubMed: 20116451]
8. Palumbo A; Dimopoulos MA; Moreau P; Chng W-J; Goldschmidt H; Hájek R; Facon T; Ludwig H; Pour L; Niesvizky R; Oriol A; Rosiñol L; Suvorov A; Gaidano G; Pika T; Weisel K; Goranova-Marinova V; Gillenwater HH; Mohamed N; Feng S; Joshua D Blood 2015, 126, (23), 1844–1844. [PubMed: 26286849]
9. Demo SD; Kirk CJ; Aujay MA; Buchholz TJ; Dajee M; Ho MN; Jiang J; Laidig GJ; Lewis ER; Parlati F; Shenk KD; Smyth MS; Sun CM; Vallone MK; Woo TM; Molineaux CJ; Bennett MK Cancer Res 2007, 67, (13), 6383–91. [PubMed: 17616698]
10. Deshaies RJ BMC Biology 2014, 12, (1), 94. [PubMed: 25385277]
11. Lamothe B; Wierda WG; Keating MJ; Gandhi V Clin Cancer Res 2016, 22, (18), 4712–4726. [PubMed: 27026200]
12. Verma R; Foster RE; Horgan K; Mounsey K; Nixon H; Smalle N; Hughes TA; Carter CR Breast cancer research : BCR 2016, 18, (1), 10. [PubMed: 26810608]
13. Litterman AJ; Zellmer DM; Grinnen KL; Hunt MA; Dudek AZ; Salazar AM; Ohlfest JR J Immunol 2013, 190, (12), 6259–6268. [PubMed: 23686484]
14. Robertson-Tessi M; El-Kareh A; Goriely A Journal of Theoretical Biology 2015, 380, 569–584. [PubMed: 26087282]
15. Kareva I; Waxman DJ; Lakka Klement G Cancer letters 2015, 358, (2), 100–106. [PubMed: 25541061]
16. Chang CL; Hsu YT; Wu CC; Lai YZ; Wang C; Yang YC; Wu TC; Hung CF Cancer Res 2013, 73, (1), 119–27. [PubMed: 23108141]
17. Ghiringhelli F; Menard C; Puig PE; Ladoire S; Roux S; Martin F; Solary E; Le Cesne A; Zitvogel L; Chauffert B Cancer Immunology, Immunotherapy 2007, 56, (5), 641–648. [PubMed: 16960692]
18. Banissi C; Ghiringhelli F; Chen L; Carpentier AF Cancer Immunology, Immunotherapy 2009, 58, (10), 1627–1634. [PubMed: 19221744]
19. Singh R; Lillard JW Experimental and molecular pathology 2009, 86, (3), 215–223. [PubMed: 19186176]
20. Jyoti A; Fugit KD; Sethi P; McGarry RC; Anderson BD; Upreti M Scientific Reports 2015, 5, 15236–15236. [PubMed: 26468877]
21. Fang RH; Kroll AV; Zhang L Small (Weinheim an der Bergstrasse, Germany) 2015, 11, (41), 5483–5496.
22. Min Y; Roche KC; Tian S; Eblan MJ; McKinnon KP; Caster JM; Chai S; Herring LE; Zhang L; Zhang T; DeSimone JM; Tepper JE; Vincent BG; Serody JS; Wang AZ Nature Nanotechnology 2017, 12, (9), 877–882.

23. Corazzari M; Gagliardi M; Fimia GM; Piacentini M Frontiers in oncology 2017, 7, 78–78. [PubMed: 28491820]
24. Lee AH; Iwakoshi NN; Anderson KC; Glimcher LH Proc Natl Acad Sci U S A 2003, 100, (17), 9946–51. [PubMed: 12902539]
25. Urra H; Dufey E; Lisbona F; Rojas-Rivera D; Hetz C Biochimica et Biophysica Acta (BBA) - Molecular Cell Research 2013, 1833, (12), 3507–3517. [PubMed: 23988738]
26. Shen G; Xing R; Zhang N; Chen C; Ma G; Yan X ACS Nano 2016, 10, (6), 5720–5729. [PubMed: 27223166]
27. Abouelmagd SA; Sun B; Chang AC; Ku YJ; Yeo Y Molecular Pharmaceutics 2015, 12, (3), 997–1003. [PubMed: 25658769]
28. Sun B; Taha MS; Ramsey B; Torregrosa-Allen S; Elzey BD; Yeo Y Journal of Controlled Release 2016, 235, (Supplement C), 91–98. [PubMed: 27238443]
29. Wang Z; Yang J; Kirk C; Fang Y; Alsina M; Badros A; Papadopoulos K; Wong A; Woo T; Bomba D; Li J; Infante JR Drug metabolism and disposition: the biological fate of chemicals 2013, 41, (1), 230–7. [PubMed: 23118326]
30. EMA/517040/2016 Group of variations including an extension of indication assessment report. https://www.ema.europa.eu/documents/variation-report/kyprolis-h-c-3790-ii-0001-g-epar-assessment-report-variation_en.pdf (Acess date: Oct 2018),
31. Tao X; Zhang Q; Ling K; Chen Y; Yang W; Gao F; Shi G PLoS ONE 2012, 7, (11), e49304. [PubMed: 23166632]
32. Khan SN; Islam B; Yennamalli R; Sultan A; Subbarao N; Khan AU European Journal of Pharmaceutical Sciences 2008, 35, (5), 371–382. [PubMed: 18762252]
33. Brewster ME; Loftsson T Advanced Drug Delivery Reviews 2007, 59, (7), 645–666. [PubMed: 17601630]
34. International Organization for Standardization 2009, ISO 10993-5.
35. Cesta MF Toxicologic pathology 2006, 34, (5), 455–65. [PubMed: 17067939]
36. Invitrogen Cell concentrations in human and mouse samples. https://assets.thermofisher.com/TFS-Assets/LSG/brochures/I-076357%20cell%20count%20table%20topp_WEB.pdf
37. Klimecki WT; Futscher BW; Grogan TM; Dalton WS Blood 1994, 83, (9), 2451. [PubMed: 7513198]
38. Gollapudi S; Gupta S Journal of Clinical Immunology 2001, 21, (6), 420–430. [PubMed: 11811787]
39. Cordon-Cardo C; O'Brien JP; Boccia J; Casals D; Bertino JR; Melamed MR Journal of Histochemistry & Cytochemistry 1990, 38, (9), 1277–1287. [PubMed: 1974900]
40. Besse A; Stolze SC; Rasche L; Weinhold N; Morgan GJ; Kraus M; Bader J; Overkleeft HS; Besse L; Driessen C Leukemia 2018, 32, (2), 391–401. [PubMed: 28676669]
41. Labieniec M; Gabryelak T Journal of photochemistry and photobiology. B, Biology 2006, 82, (1), 72–8.
42. Van Buren JP; Robinson WB Journal of Agricultural and Food Chemistry 1969, 17, (4), 772–777.
43. Mehrara E; Forssell-Aronsson E; Ahlman H; Bernhardt P Cancer Research 2007, 67, (8), 3970. [PubMed: 17440113]
44. Lechner MG; Karimi SS; Barry-Holson K; Angell TE; Murphy KA; Church CH; Ohlfest JR; Hu P; Epstein AL Journal of immunotherapy (Hagerstown, Md. : 1997) 2013, 36, (9), 477–489.
45. Castle JC; Loewer M; Boegel S; de Graaf J; Bender C; Tadmor AD; Boisguerin V; Bukur T; Sorn P; Paret C; Diken M; Kreiter S; Türeci Ö; Sahin U BMC Genomics 2014, 15, (1), 190. [PubMed: 24621249]
46. Casares N; Pequignot MO; Tesniere A; Ghiringhelli F; Roux S; Chaput N; Schmitt E; Hamai A; Hervas-Stubbs S; Obeid M; Coutant F; Métivier D; Pichard E; Aucouturier P; Pierron G; Garrido C; Zitvogel L; Kroemer G The Journal of experimental medicine 2005, 202, (12), 1691. [PubMed: 16365148]
47. Baghdadi M; Chiba S; Yamashina T; Yoshiyama H; Jinushi M PLoS ONE 2012, 7, (6), e39607–e39607. [PubMed: 22761839]

48. Aaes Tania L.; Kaczmarek A; Delvaeye T; De Craene B; De Koker S; Heyndrickx L; Delrue I; Taminau J; Wiernicki B; De Groote P; Garg Abhishek D.; Leybaert L; Grooten J; Bertrand Mathieu J. M.; Agostinis P; Berx G; Declercq W; Vandenabeele P; Krysko Dmitri V. Cell Reports 2016, 15, (2), 274–287. [PubMed: 27050509]

49. Lin Y-C; Chang L-Y; Huang C-T; Peng H-M; Dutta A; Chen T-C; Yeh C-T; Lin C-Y The Journal of Immunology 2009, 182, (10), 6095. [PubMed: 19414761]

50. Chiarella P; Bruzzo J; Meiss RP; Ruggiero RA Cancer letters 2012, 324, (2), 133–141. [PubMed: 22634498]

51. Huang AY; Gulden PH; Woods AS; Thomas MC; Tong CD; Wang W; Engelhard VH; Pasternack G; Cotter R; Hunt D; Pardoll DM; Jaffee EM Proceedings of the National Academy of Sciences of the United States of America 1996, 93, (18), 9730–9735. [PubMed: 8790399]

52. Gallina G; Dolcetti L; Serafini P; De Santo C; Marigo I; Colombo MP; Basso G; Brombacher F; Borrello I; Zanovello P; Bicciato S; Bronte V The Journal of clinical investigation 2006, 116, (10), 2777–2790. [PubMed: 17016559]

53. Kano A Scientific Reports 2015, 5, 8913–8913. [PubMed: 25746680]

54. Chan T-S; Hsu C-C; Pai VC; Liao W-Y; Huang S-S; Tan K-T; Yen C-J; Hsu S-C; Chen W-Y; Shan Y-S; Li C-R; Lee MT; Jiang K-Y; Chu J-M; Lien G-S; Weaver VM; Tsai KK The Journal of experimental medicine 2016, 213, (13), 2967–2988. [PubMed: 27881732]

55. Klement G; Baruchel S; Rak J; Man S; Clark K; Hicklin DJ; Bohlen P; Kerbel RS J Clin Invest 2000, 105, (8).

56. Browder T; Butterfield CE; Kräling BM; Shi B; Marshall B; O'Reilly MS; Folkman J Cancer Research 2000, 60, (7), 1878. [PubMed: 10766175]

57. Williams S; Pettaway C; Song R; Papandreou C; Logothetis C; McConkey DJ Molecular Cancer Therapeutics 2003, 2, (9), 835. [PubMed: 14555702]

58. Roccaro AM; Hideshima T; Raje N; Kumar S; Ishitsuka K; Yasui H; Shiraishi N; Ribatti D; Nico B; Vacca A; Dammacco F; Richardson PG; Anderson KC Cancer Research 2006, 66, (1), 184. [PubMed: 16397231]

59. Sanchez E; Li M; Wang CS; Tang G; Gillespie A; Chen H; Berenson JR Leukemia Research 2017, 57, 45–54. [PubMed: 28288323]

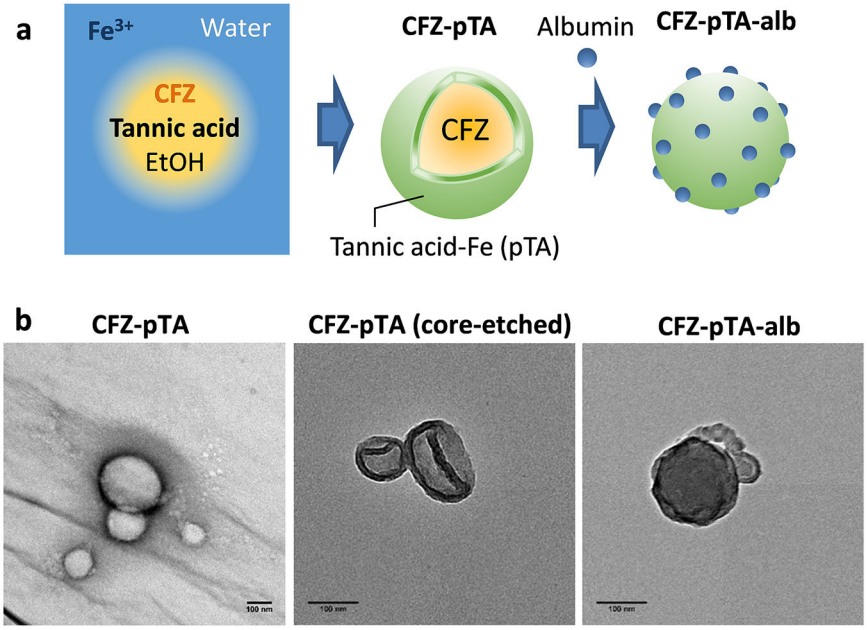

Figure 1.

(a) Schematic description of the CFZ-pTA preparation by TA/Fe^{3+} interfacial assembly formation and CFZ-pTA-alb with albumin coating. (b) TEM images of CFZ-pTA, CFZ-pTA with the CFZ core etched, and CFZ-pTA-alb. Scale bars: 100 nm.

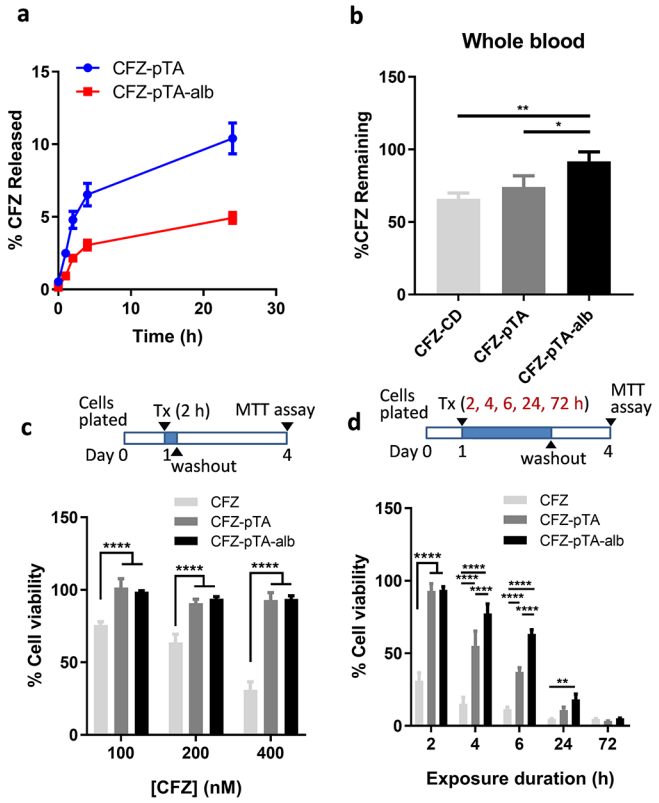

Figure 2.

Albumin coating as a barrier to CFZ release from CFZ-pTA-alb. (a) *In vitro* release kinetics of CFZ-pTA and CFZ-pTA-alb in 10% FBS/RPMI medium. (b) *In vitro* stability of CFZ-CD, CFZ-pTA, and CFZ-pTA-alb after incubation at 37 °C in whole blood for 30 min. *: $p < 0.05$, **: $p < 0.01$ and ****: $p < 0.0001$, one-way ANOVA with Tukey's multiple comparisons test. (c) Viability of B16F10 cells exposed to unformulated CFZ (CFZ dissolved in DMSO), CFZ-pTA or CFZ-pTA-alb at concentrations equivalent to CFZ 100, 200 or 400 nM for 2 h, followed by incubation in drug-free medium with the total incubation time of 72 h. (d) Viability of B16F10 cells exposed to unformulated CFZ, CFZ-pTA or CFZ-pTA-alb at 400 nM CFZ-equivalent for 2, 4, 6, 24 or 72 h, followed by incubation in drug-free medium with the total incubation time of 72 h. ***: $p < 0.001$ and ****: $p < 0.0001$, two-way ANOVA with Tukey's multiple comparisons test or Dunnett's multiple comparisons test versus unformulated CFZ.

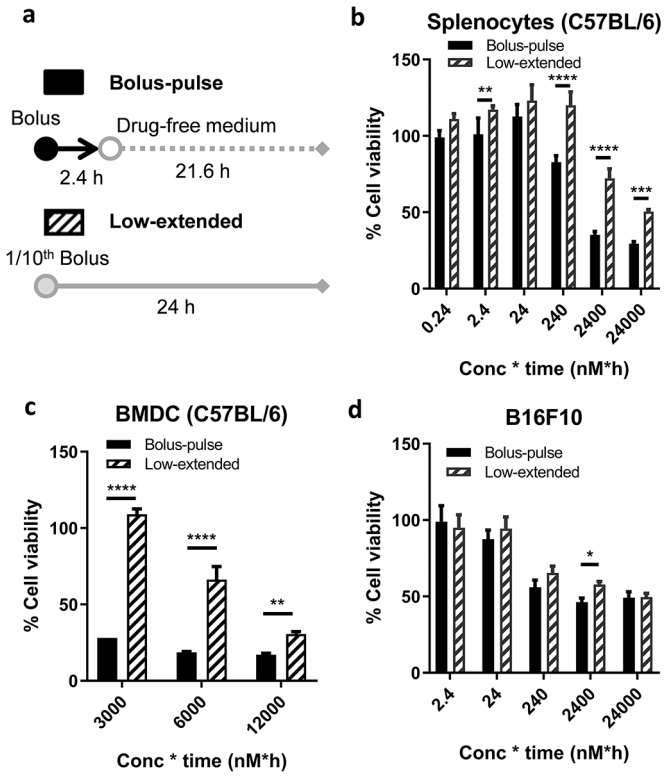

Figure 3.

Comparison of a pulse treatment of bolus dose (bolus-pulse) vs. an extended treatment of low dose (low-extended). Bolus-pulse: Cells were incubated with unformulated CFZ at different CFZ concentrations for 2.4 h then washed and incubated in drug-free medium for additional 21.6 h making the total incubation time of 24 h. Low-extended: Cells were incubated with at $1/10^{th}$ CFZ concentrations for 24 h. Cell viability was measured by the MTT assay at the end of 24 h. % cell viability was calculated by normalizing to the viability of control cells treated with the equivalent amount of vehicle for the same period of time. X-axis = CFZ concentration × exposure time (e.g., 2.4 = 1 nM for 2.4 h followed by incubation in drug-free medium for 21.6 h or 0.1 nM for 24 h). (a) Schematic description of two dosing regimens. Viability of (b) splenocytes from C57BL/6 mice, (c) dendritic cells derived from C57BL/6 mouse bone marrow and (d) B16F10 cells. *: $p < 0.05$, **: $p < 0.01$, ***: $p < 0.001$ and ****: $p < 0.0001$, by two-way ANOVA with Sidak's multiple comparisons test.

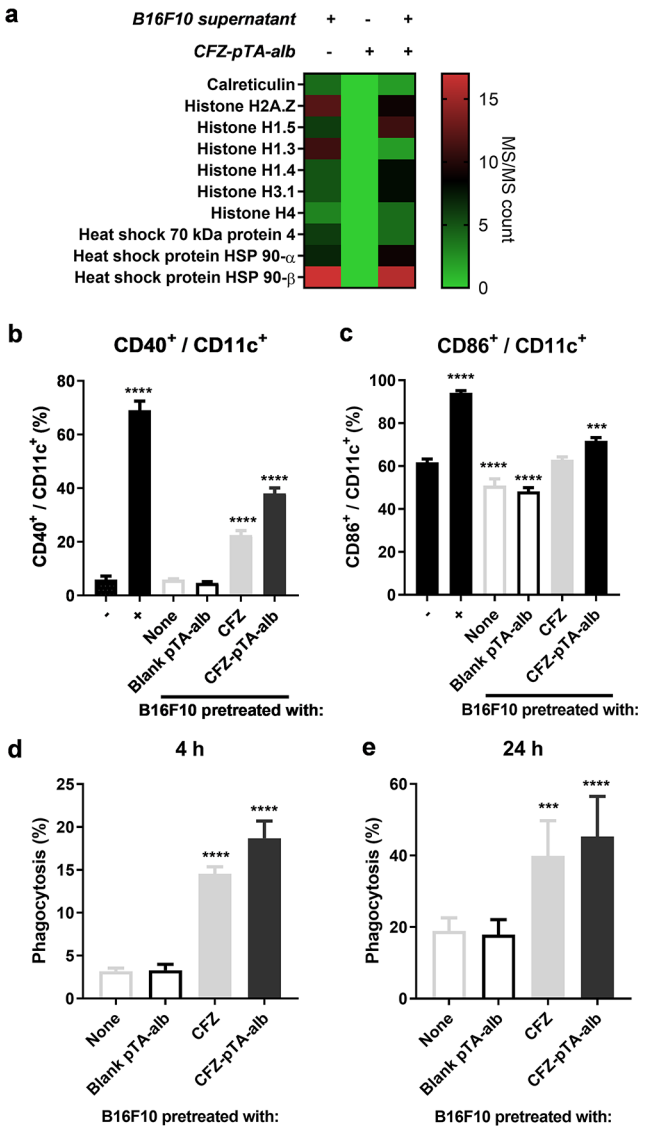

Figure 4.

Nanocapsules capture DAMPs from dying tumor cells and activate DCs: (a) Spectral counts of proteins, analyzed by LC-MS/MS, in the supernatant of B16F10 cells treated with 10 μM CFZ in serum-free medium (B16F10 supernatant), CFZ-pTA-alb (1 mg/mL NP), CFZ-pTA-alb (1 mg/mL NP) incubated in the B16F10 supernatant for 2 h at 37 °C and then rinsed. (b and c) BMDC activation following coculture with B16F10 cells pretreated with unformulated CFZ, CFZ-pTA-alb (200 nM CFZ-equivalent) or blank pTA-alb for 24 h, indicated by the expression of (b) CD40 and (c) CD86 on $CD11c^+$ BMDCs. −: non-activated BMDCs; +: LPS-activated BMDCs. ***: $p < 0.001$ and ****: $p < 0.0001$, one-way ANOVA with Dunnett's multiple comparison's test versus non-activated BMDCs. (d and e) Phagocytosis of B16F10 cells by BMDCs: B16F10 cells were prelabeled with DiI, treated with unformulated CFZ, CFZ-pTA-alb (10 μM CFZ-equivalent) or blank pTA-alb, rinsed once and cocultured with BMDCs for (d) 4 h or (e) 24 h. BMDCs were identified with APC anti-mouse CD11c antibody and analyzed by flow cytometry. Phagocytosis (%): % of DiI^+

$CD11c^+$ cells in total $CD11c^+$ cells. ***: $p < 0.001$ and ****: $p < 0.0001$, one-way ANOVA with Dunnett's multiple comparisons test versus non-pretreated B16F10 cells.

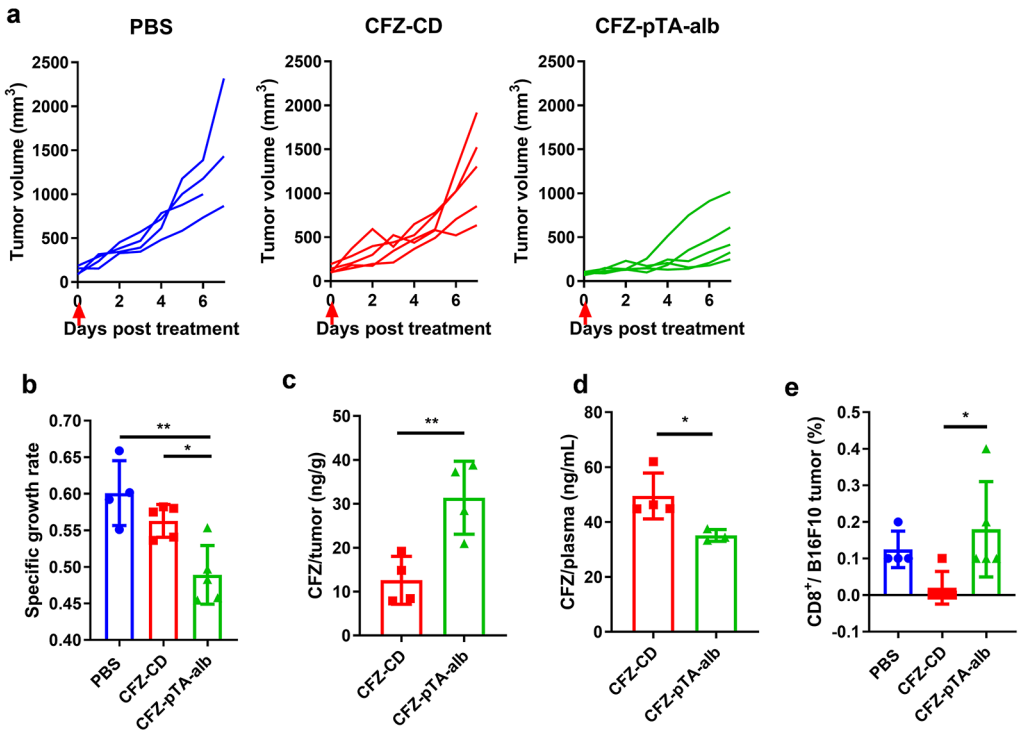

Figure 5.

The effect of CFZ-pTA-alb vs. CFZ-CD, administered as a single intratumoral (IT) injection at 1.2 μg CFZ equivalent, on B16F10@C57BL/6 mice. (a) Individual growth curves of tumors treated with PBS (n=4), CFZ-CD (n=5) or CFZ-pTA-alb (n=5). Arrow indicates the time of treatment. (b) Specific growth rate of B16F10 tumor (ΔlogV/Δt, V: tumor volume and t: time in days). *: $p<0.05$ and **: $p<0.01$, one-way ANOVA with Tukey's multiple comparisons test. (c) CFZ content in B16F10 tumors and (d) CFZ concentration in plasma collected at 2 h after IT injection of CFZ-CD (n=4) or CFZ-pTA-alb (n=4) at 1.2 μg CFZ equivalent. *: $p<0.05$ and **: $p<0.01$, unpaired two-tailed *t*-test. (e) % B16F10 tumor-infiltrating $CD8^+$ T cells determined by flow cytometry at day 7 post-treatment. *: $p<0.05$, one-way ANOVA with Tukey's multiple comparisons test.

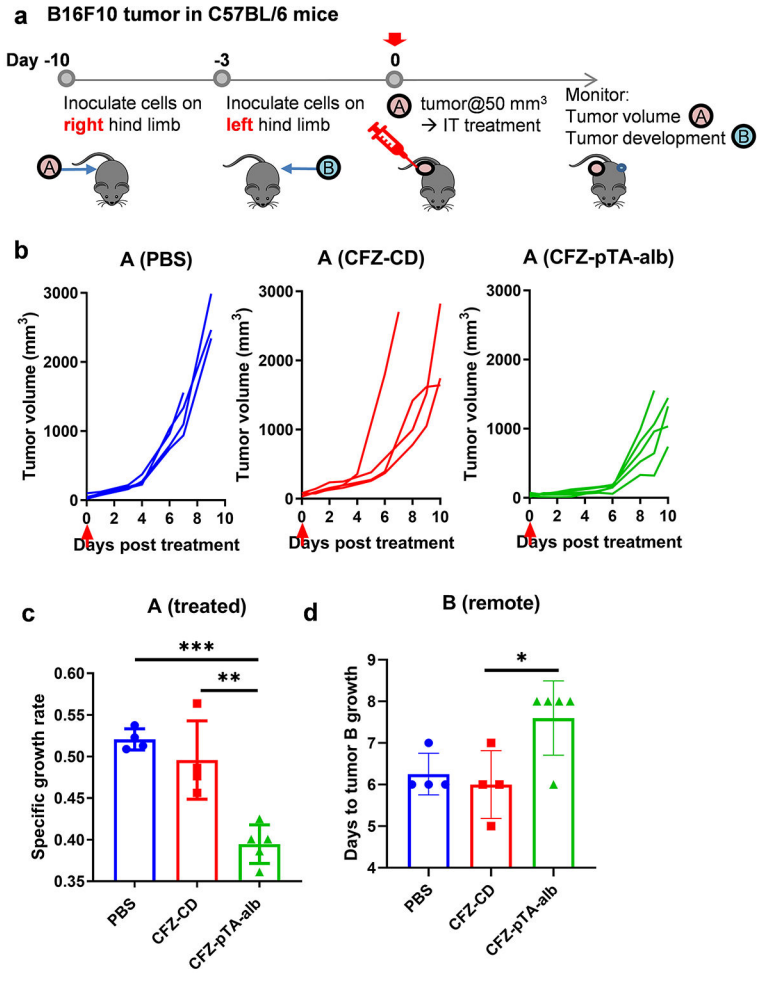

Figure 6.

The effect of CFZ-pTA-alb vs. CFZ-CD, administered as a single IT injection at 60 μg CFZ equivalent, on the treated (A) and remote (B) tumors in an immunocompetent B16F10@C57BL/6 mouse model. (a) Schedule of B16F10 tumor inoculation in C57BL/6 mice and treatment injection. (b and c) Antitumor activity in the treated tumor A: (b) Individual growth curves of tumors treated with PBS (n=4), CFZ-CD (n=4) or CFZ-pTA-alb (n=5). Arrow indicates the treatment time. (c) Specific growth rate of treated tumor (ΔlogV/Δt). (d) Days to appearance of tumor B (remote, untreated). *: $p<0.05$, **: $p<0.01$ and *** $p<0.001$, one-way ANOVA with Tukey's multiple comparisons test.

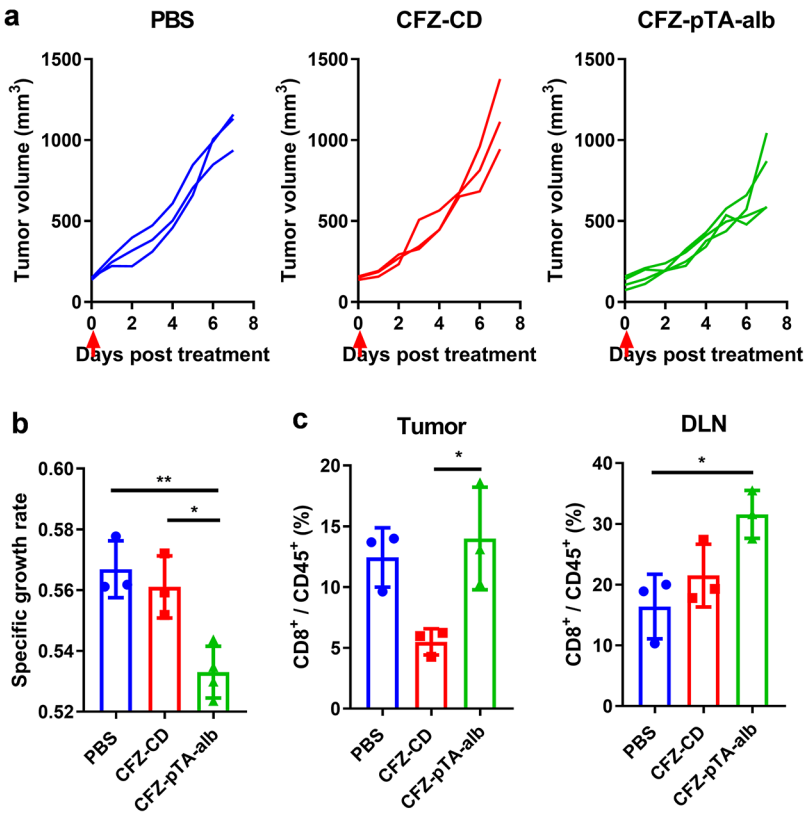

Figure 7.

The effect of CFZ-pTA-alb vs. CFZ-CD, administered as a single IT injection, on CT26@Balb/c mice. (a) Individual growth curves of tumors treated with PBS (n=3), CFZ-CD (n=3) or CFZ-pTA-alb (n=4) at 1.2 μg CFZ equivalent. Arrows indicate the treatment time. (b) Specific growth rate of CT26 tumor (ΔlogV/Δt). (c) % $CD8^+$ T cells of $CD45^+$ cells in CT26 tumors or draining lymph nodes of mice receiving a single IT injection of CFZ-CD or CFZ-pTA-alb (n=3 per group) at 60 μg CFZ equivalent, 6 days post treatment. *: $p<0.05$ and ** $p<0.01$, one-way ANOVA with Tukey's multiple comparisons test.

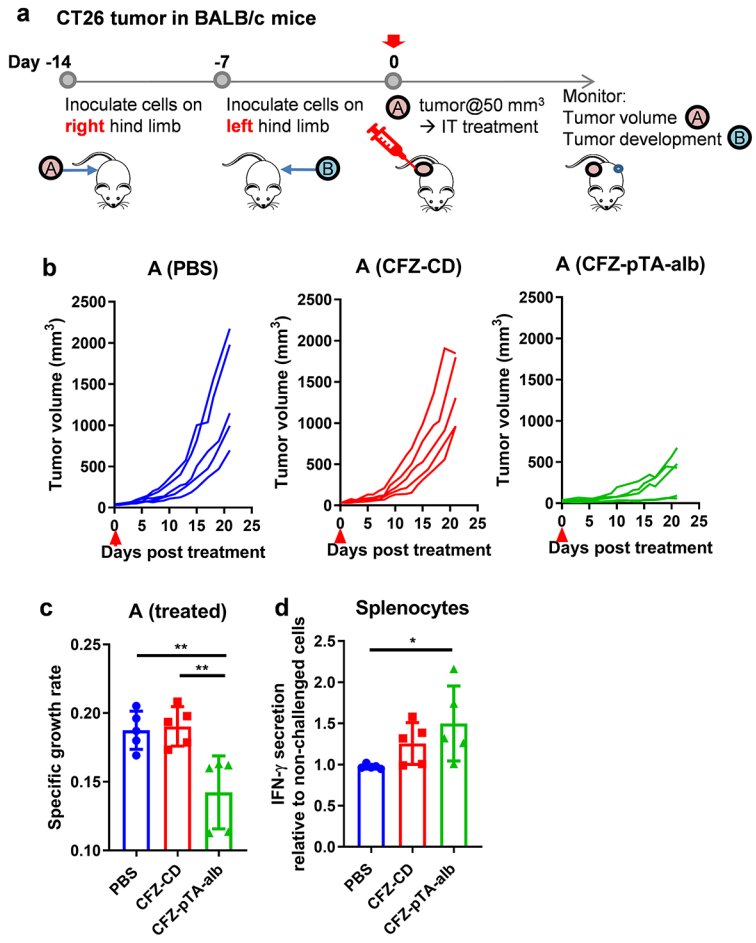

Figure 8.

The effect of CFZ-pTA-alb vs. CFZ-CD, administered as a single IT injection at 60 μg CFZ equivalent, on the treated (A) and remote (B) tumors in an immunocompetent CT26@Balb/c mouse model. (a) Schedule of CT26 tumor inoculation in Balb/c mice and treatment injection. (b and c) Antitumor activity in the treated tumor A: (b) Individual growth curves of tumors treated with PBS, CFZ-CD or CFZ-pTA-alb (n=5 per group). Arrow indicates the treatment time. (c) Specific growth rate of treated tumor (ΔlogV/Δt). (d) IFN-γ secretion from splenocytes of the mice sacrificed on day 22 post-treatment, in response to AH1 peptide, a CT26 immunodominant MHC class-I restricted antigen. IFN-γ secretion is presented relative to the basal level of IFN-γ in non-challenged splenocytes. *: $p<0.05$ and **: $p<0.01$, one-way ANOVA with Tukey's multiple comparisons test.